Article

Not peer-reviewed version

Wearables-Enhanced Support of ML-Based Movement Assessment for Distinguishing Correct from Incorrect Movement and Enabling Explainable Feedback

Georgios Bouchouras *, Georgios Sofianidis, Evangelos Kontaxakis, Konstantinos Kotis *

Posted Date: 20 April 2026

doi: 10.20944/preprints202604.1435.v1

Keywords: movement-quality assessment; wearable sensors; inertial measurement units; IMU; rehabilitation monitoring; early error detection; interpretable features

 doi:10.20944/preprints202604.1435.v1

Article

Wearables-Enhanced Support of ML-Based Movement Assessment for Distinguishing Correct from Incorrect Movement and Enabling Explainable Feedback

Georgios Bouchouras [1,2,*], Georgios Sofianidis [2], Evangelos Kontaxakis [2] and Konstantinos Kotis [1,*]

[1] Intelligent Systems Lab, Department of Cultural Technology and Communication, University of the Aegean, Mytilene 81100, Greece
[2] Center of Interdisciplinary Education and Research in Rehabilitation, Metropolitan College, Thessaloniki 54625, Greece
* Correspondence: gbouchouras@aegean.gr (G.B.); kotis@aegean.gr (K.K.)

Featured Application

The study shows that ML-based wearable movement assessment can distinguish correct from incorrect movement, explain why the movement is wrong, remain useful with fewer Inertial Measurement Units (IMUs), and support a proof-of-concept path toward corrective feedback.

Abstract

Wearable systems for rehabilitation monitoring often rely on complex sensor configurations and produce outputs that are difficult to interpret. This limits their practical use. This study investigates whether movement-quality assessment can be achieved accurately and transparently using a reduced set of signals. Using wearable sensor data from lower-limb rehabilitation tasks performed under correct and intentionally erroneous conditions, we extracted a small set of rotation-based features and evaluated them within a supervised ML framework. The results show that these features can reliably distinguish correct from incorrect movement, with classification accuracy around 0.70, while preserving clear biomechanical interpretation. Reduced sensor configurations retained, and in some cases improved, performance, with balanced accuracy reaching 0.947 and 0.917 in the examined tasks. A proof-of-concept real-time formulation further showed that movement deviations can be detected early within repetitions, while limiting false feedback on correct executions to approximately 9%. Overall, the findings show that movement-quality assessment can be achieved with minimal sensing, while also supporting early error detection and practical feedback. These properties are relevant to wearable rehabilitation systems, including IoT applications that depend on efficient sensing, interpretable analysis, and timely feedback.

Keywords: movement-quality assessment; wearable sensors; inertial measurement units; IMU; rehabilitation monitoring; early error detection; interpretable features

1. Introduction

Assessing movement quality is an important task in rehabilitation monitoring. Clinicians need not only to detect altered movement, but also to understand how and why it deviates from the intended pattern. Wearable sensing systems can help address this need. They combine wearable sensors with computational analysis of collected sensor data to support clinician review, patient feedback, and remote follow-up. Their value is especially clear in home-based rehabilitation, where frequent in-person assessment is difficult and low-burden monitoring is needed [1,3]. Recent studies have shown growing interest in combining inertial sensing with machine learning (ML) to extend rehabilitation assessment beyond the clinic [7,8].

 doi:10.20944/preprints202604.1435.v1

These developments are also relevant to applications of artificial intelligence (AI) in Internet of Things (IoT) environments. In such settings, wearable devices can support continuous monitoring and data-driven decision-making. However, practical deployment depends on more than predictive accuracy alone. Sensor complexity, usability, and interpretability also matter. These factors influence user acceptance and long-term use in healthcare applications [25].

Despite the progress in the field, two main challenges remain. The first is sensors burden. Multi-sensor configurations can capture detailed movement information, but they are harder to use in routine care or home settings because they require extra configuration and deployment effort. Simpler configurations are easier to deploy, but they may miss movement variations that are distributed across several body segments. The second challenge is interpretability. Many models can detect movement deviations, but they do not clearly indicate (explain to decision makers) what has actually changed. This limits their value for clinical interpretation and patient-facing feedback [2]. In practice, useful systems should reduce sensing complexity while still producing meaningful and understandable outputs.

In this study, we investigate whether movement-quality assessment can be achieved with a reduced set of signals derived from wearable sensors/inertial measurement units (IMUs). Using data from lower-limb rehabilitation exercises performed under correct and instructed erroneous conditions, we apply an ML framework to analyse and understand movement discrimination, sensor reduction, interpretability, and feedback-oriented monitoring. We also extend the analysis to a proof-of-concept setting for early error detection and feedback based on short time windows. The proposed approach combines efficient IMU-based sensing, ML, and readable feature-based outputs to advance practical wearable systems for rehabilitation.

The objectives of this study are the following:

1. Distinguish correct from incorrect (altered) movement signals using simple and interpretable measures;
2. Provide explainability output regarding the reasons the movement is altered, using the same set of measures;
3. Identify smaller sensor sets that are more suitable for wearable system deployment;
4. Test whether this approach can support a simulated real-time corrective-feedback setting.

The paper is structured as follows: Section 2 (Materials and Methods) presents the dataset, preprocessing pipeline, feature extraction, subject-level aggregation, and the statistical and ML analyses used in this study. Section 3 (Results) reports the main findings, including effect size analysis, classification performance, and sensitivity analyses. Section 4 (Discussion) interprets the results, highlights the clinical and methodological implications, and addresses the limitations of the study. Finally, Section 5 (Conclusions) summarizes the main contributions and outlines directions for future work.

2. Materials and Methods

2.1. Dataset and Tasks

We analyzed GAITEX, a publicly available dataset of impaired gait and rehabilitation exercises recorded with inertial and optical sensors [4,5]. We focused on two unilateral lower-limb tasks derived from Xsens (wearable motion-capture system [6]) body-segment orientations. The repeated dynamic task (RD) contained the labels `rd_correct`, `rd_pronation`, `rd_supination`, and `rd_toes`. The right-leg stance task (RGS) contained `rgs_correct`, `rgs_abduction`, `rgs_flexion`, and `rgs_stork`. After preprocessing and subject-level aggregation, 19 subjects were available for RD and 18 for RGS.

The two rehabilitation tasks analyzed in this study are illustrated in Figure 1. Both exercises are performed in a standing position and were designed to probe lower-limb control under clinically relevant conditions. The repeated dynamic task (RD) consists of a cyclic lower-limb movement emphasizing controlled ankle and foot motion. The right-leg stance task (RGS) focuses on postural stability while balancing on the right leg and controlling compensatory body movements. For each task, the dataset provides a standardized start position, one correct execution, and three representative

 doi:10.20944/preprints202604.1435.v1

erroneous movement patterns commonly observed in individuals with foot drop. These task variants form the basis for the movement-quality analyses performed in this study.

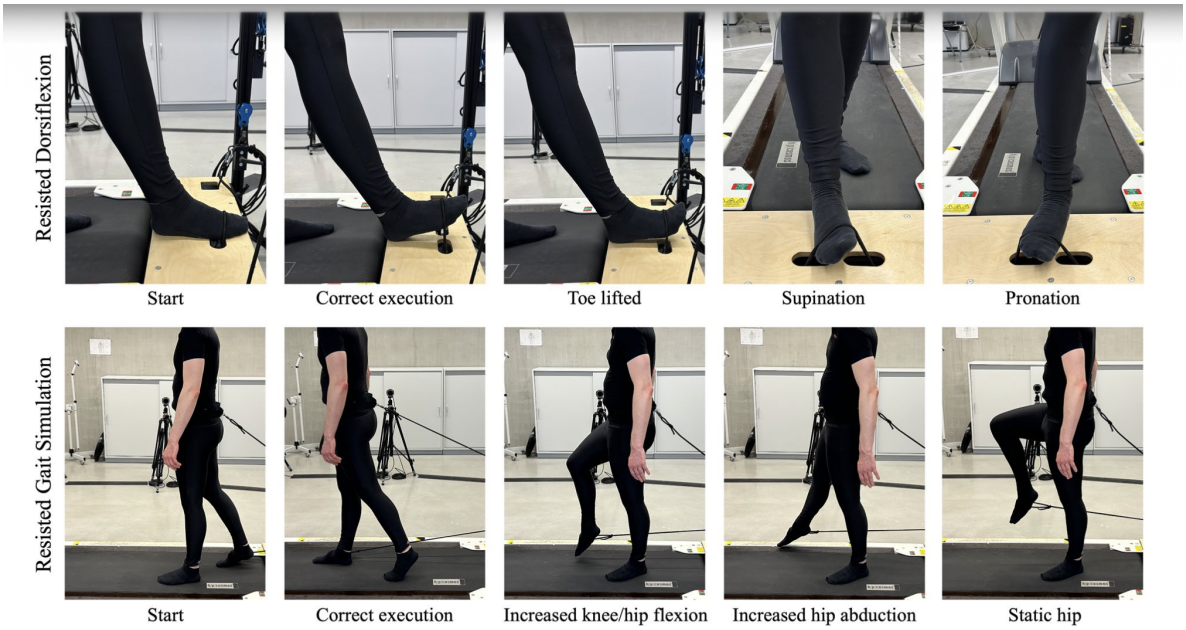

Figure 1. Overview of the two rehabilitation tasks and their execution variants, adapted from Spilz et al. (2025) [4]. Both exercises are performed in a standing position. The repeated dynamic task (RD) is shown in the upper row, and the right-leg stance task (RGS) in the lower row. For each task, the first image illustrates the standardized start position, followed by the correct execution and three representative erroneous movement patterns commonly observed in individuals with foot drop.

2.2. Feature Extraction

For each repetition and each instrumented segment, quaternions were re-normalized and converted into rotation-step magnitudes Figure 2. From these time series, we extracted five interpretable rotational features:

- mean angular speed
- RMS angular speed
- peak angular speed
- RMS angular acceleration
- rotational range.

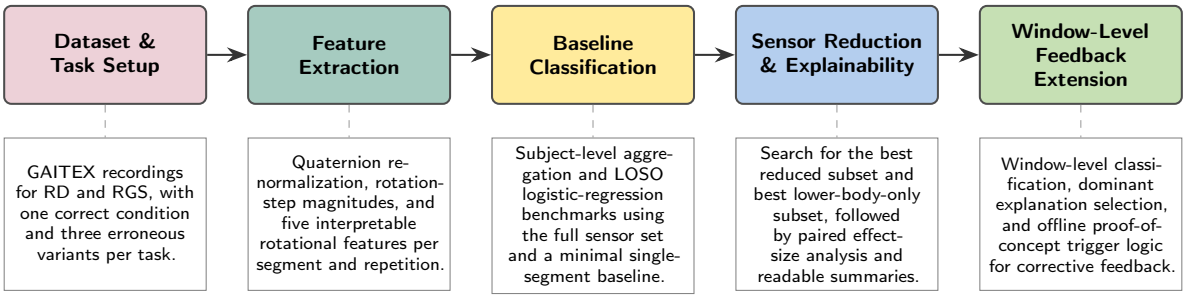

Figure 2. Overview of the proposed workflow. The study starts from GAITEX rehabilitation tasks, extracts interpretable rotational IMU features, evaluates subject-level correct-versus-incorrect movement classification, identifies task-specific reduced sensor configurations and readable explanations, and extends the analysis to an offline proof-of-concept window-level feedback setting.

We intentionally kept the feature set simple. No latent embeddings, spectral transforms, or deep learned features were used. This served two purposes. First, it allowed us to test whether

 doi:10.20944/preprints202604.1435.v1

straightforward kinematic summaries were already sufficient for useful discrimination between correct and incorrect movement. Second, it supported later interpretation, because model behavior could be related directly to segment-level biomechanical quantities rather than to hidden latent variables [8,21]. Repetition-level features were then averaged to the subject level separately for each subject, task, condition, and segment. Each subject-level sample therefore represents the average feature profile for one subject under one task condition.

2.3. ML Pipeline

The ML component of the study was implemented as a supervised pipeline operating on the interpretable segment-level feature tables. For the binary movement-quality task, the target label was *correct* versus *incorrect* movement, where the incorrect class pooled the three instructed erroneous variants within each task. For the retained multiclass benchmark, the target label was the four-condition task label consisting of the correct condition plus the three specific erroneous variants.

We used logistic regression as the classifier because it is appropriate for small tabular datasets, yields directly auditable linear decision functions, and keeps the relation between learned model behavior and the underlying feature space transparent. Unless stated otherwise, each classification pipeline used median imputation for missing values, z-score standardization, and logistic regression with the `liblinear` solver and `max_iter = 5000`. Performance was estimated with leave-one-subject-out (LOSO) cross-validation so that each test fold contained data from a subject not used for model fitting.

For binary movement-quality classification, we report accuracy and balanced accuracy. For the retained multiclass benchmark, we report accuracy. Classification was performed by the logistic-regression model, whereas interpretation was derived directly from the same kinematic features used for classification.

2.4. Baseline Benchmarks

The baseline analysis began with subject-level benchmarking using the full sensor set. Binary discrimination between correct and incorrect movement was evaluated with the logistic-regression pipeline described above under LOSO cross-validation. This full sensor set benchmark was compared with a minimal single-segment baseline, defined as the simplest one-segment representation used as a low-information reference point.

We also retained a multiclass LOSO benchmark using the same model family to test whether the same interpretable feature space preserved information about the specific erroneous variant type. These baseline analyses establish the first methodological question clearly: do interpretable IMU features separate correct from incorrect movement before any sensor-reduction step is introduced?

2.5. Sensor Configuration Analysis

To study the trade-off between sensing burden and analytical performance, we evaluated many sensor subsets of size 1 to 4 for each task. For every subset, we:

1. built a subject-level wide feature table from the selected segments;
2. trained a binary logistic-regression model with median imputation, z-score standardization, the `liblinear` solver, and `max_iter = 5000`;
3. evaluated LOSO accuracy and balanced accuracy.

For each sensor count, we retained the best-performing subset according to mean LOSO balanced accuracy. Throughout the paper, we refer to these as the *best reduced subsets*. We report two versions of this analysis:

- an unconstrained analysis across all available segments;
- a lower-body-only analysis including feet, lower legs, upper legs, and pelvis.

 doi:10.20944/preprints202604.1435.v1

The unconstrained analysis identifies which segments carry the most information for movement-quality classification. The lower-body-only analysis identifies the best lower-body-only subset, which is more realistic for wearable rehabilitation or home-monitoring use.

2.6. Explainability and Readable Feedback Layer

We also added an explainability layer based on the same interpretable feature space used for classification. For each task variant, we computed segment-feature deviations relative to the correct condition using subject-level paired differences and paired effect sizes (d_z). We then translated the strongest deviations into short natural-language summaries, such as "higher typical rotational speed at the right lower leg" or "lower rotational speed at the left foot."

We generated two forms of summaries. First, we produced variant-level summaries describing the dominant deviations associated with each erroneous condition. Second, we generated subject-specific example summaries relative to each subject's own correct baseline.

This layer was deliberately kept simple. It was designed to be readable by humans and suitable for future reporting tools, not to serve as a validated conversational feedback system. The explainability claim in this study is therefore specific: the same interpretable segment-feature space used for movement-quality classification can also indicate which body region and which movement quantity changed most strongly in each variant. In a wearable monitoring setting, that kind of output could support dashboards, clinician summaries, or future feedback interfaces without relying on opaque model behavior alone.

2.7. Proof-of-Concept Closed-Loop Extension

To extend the methodology, we reformulated the same tasks at the window level. Each repetition was segmented into overlapping windows, and the same five interpretable rotational features were extracted per segment and per window. Window-level feature tables were then built for three sensor configurations per task:

- the full sensor set;
- the best reduced subset from the subject-level unconstrained search;
- the best lower-body-only subset from the subject-level constrained search.

For each window-level sensor configuration, we trained binary logistic-regression models with LOSO cross-validation using the same preprocessing logic as in the subject-level analysis. This allowed us to test whether correct-versus-incorrect discrimination remained available before the full repetition had ended. We summarized this stage using window-level accuracy, window-level balanced accuracy, and median first-detect progress within incorrect repetitions.

We then derived a window-level explanation layer. For windows predicted as incorrect, each segment-feature value was compared with its task-specific correct reference. The dominant explanation for a window was defined as the segment-feature deviation with the largest standardized departure from the correct condition. This yielded interpretable keys such as `LowerLeg Right + mean speed + higher` or `Pelvis + mean speed + higher`. Variant-level summaries were then obtained by aggregating the most frequent dominant explanation across incorrect windows.

Finally, we simulated a simple corrective-feedback trigger. A cue was triggered only when three conditions were met: the window was predicted as incorrect, the incorrect-class probability exceeded a threshold, and the same dominant explanation persisted for at least three consecutive windows. Because the default trigger was too sensitive, we retained a more conservative tuned rule for reporting: RD used a probability threshold of 0.90 and a deviation-score threshold of 2.5, whereas RGS used 0.95 and 1.5, respectively. This proof-of-concept extension was evaluated as an offline replay of a possible closed-loop policy rather than as a live hardware deployment.

The code (re)used for this study is publicly available in the GitHub repository at Machine-Learning-with-Minimal-IMUs (accessed on 13 April 2026). The repository includes the scripts used for data loading, repetition segmentation, interpretable feature extraction, subject-level movement-quality

 doi:10.20944/preprints202604.1435.v1

classification, sensor- subset evaluation, readable explainability outputs, and the proof-of-concept window-level feedback extension. It also includes a README file that explains the repository structure, software requirements, expected data layout, and the main steps needed to reproduce the analyses.

3. Results

3.1. Baseline Results

The baseline analyses showed that the feature set contained useful movement-quality information. Full representations outperformed minimal single-segment baselines for both tasks. In RD, mean LOSO accuracy was 0.697 for the full representation and 0.447 for the minimal representation ($\Delta = 0.25$, sign-flip $p < 0.001$). In RGS, the corresponding values were 0.694 and 0.472 ($\Delta = 0.222$, $p = 0.003$).

Multiclass LOSO classification remained above chance in both tasks, with mean accuracy 0.461 in RD and 0.403 in RGS (chance = 0.25). This means that the same simple features also retain some information about which variant was performed. The baseline summary is shown in Table 1.

Table 1. Baseline subject-level benchmarks. Binary results compare full and minimal representations. Multiclass accuracy refers to four-class LOSO classification (correct plus three variants).

Task	Full acc.	Minimal acc.	Δ (Full−Min.)	Multiclass acc.
RD	0.697	0.447	0.250 ($p < 0.001$)	0.461
RGS	0.694	0.472	0.222 ($p = 0.003$)	0.403

Figure 3 shows the segment-ablation results. It highlights that classification performance is not uniform across body regions and that the most informative segments differ between RD and RGS. This supports the practical conclusion that sensor placement should be task-specific.

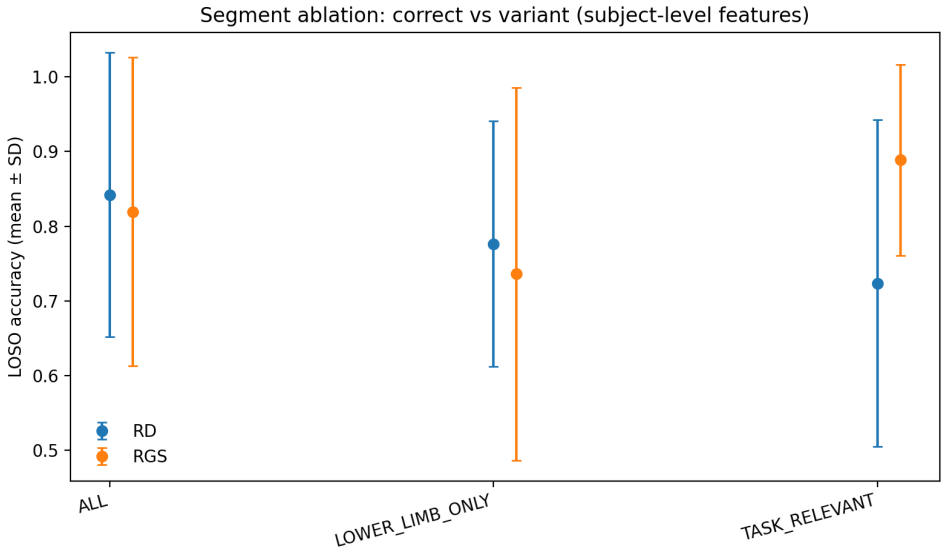

Figure 3. Segment-ablation results for subject-level binary classification. Performance differs across body regions, indicating that the most informative segments depend on the task.

3.2. Explainable Results and Readable Movement Summaries

The explainability layer converted the strongest segment-feature changes into short movement summaries. The point here is not that the system produces generic text, but that the text is anchored in concrete, task-specific kinematic deviations from the correct condition. In RD pronation, the clearest pattern was higher right lower-leg speed across mean, RMS, and peak metrics ($d_z = 1.79$–1.87). In RD toes, the strongest changes shifted to the right hand, where peak speed and rotational range exceeded $d_z = 2.3$, suggesting a strong compensatory arm response. In RGS abduction, the dominant pattern was

 doi:10.20944/preprints202604.1435.v1

reduced left-foot speed together with increased pelvis speed. In RGS stork, the pattern combined left-foot reductions with increased right upper-leg motion. These are interpretable movement fingerprints rather than opaque importance scores [21].

These summaries do not replace expert interpretation, but they show why the study makes a limited explainability claim. The same feature space used for classification also identifies which segment and which rotational quantity changed most strongly in each variant, and those changes can be rendered in language without leaving the interpretable feature domain. In practice, they can be used either as direct machine-generated explanations or as structured input for future reporting tools in wearable system platforms. Representative text outputs are listed in Table 2.

Table 2. Examples of readable movement summaries generated from the strongest segment-feature deviations.

Variant	Readable Summary
RD pronation	Very large increases in right lower-leg typical, average, and peak rotational speed.
RD supination	Very large increases in right-hand typical and average rotational speed, plus increased right lower-leg rotational excursion.
RD toes	Very large increases in right-hand peak rotational speed, rotational excursion, and typical rotational speed.
RGS abduction	Very large reductions in left-foot rotational speed with simultaneous pelvis speed increase.
RGS flexion	Marked reductions in left-foot speed and lower left-leg mean speed.
RGS stork	Increased right upper-leg mean speed with strong reductions in left-foot speed metrics.

The readable summaries are also consistent with the feature-relevance analysis in Figure 4. These task-specific maps support the same explainability point: the strongest discriminative patterns are localized to interpretable segment-feature combinations rather than hidden latent factors. In other words, the explanation layer is not an extra cosmetic addition after classification; it is derived from the same transparent structure that makes the classifier output auditable in the first place.

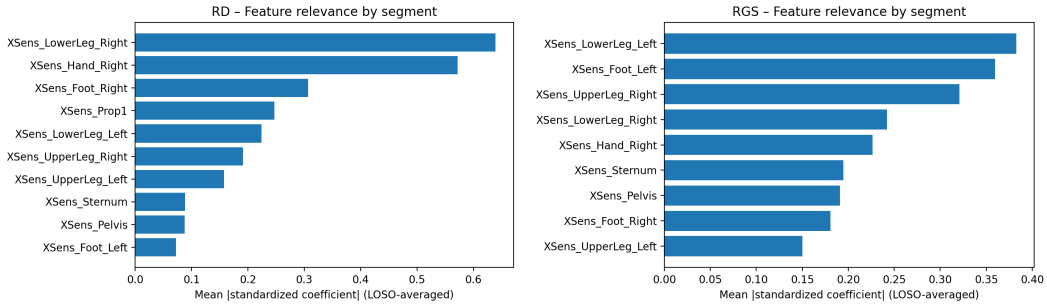

(**a**) RD feature relevance. (**b**) RGS feature relevance.

Figure 4. Feature-relevance maps for RD and RGS retained from the earlier analysis. The maps highlight which segment-feature combinations contributed most strongly to discrimination in each task.

3.3. Sensor Configuration Results

The sensor-subset analysis addressed the third question of the study: how many sensors are actually needed once correct-versus-incorrect discrimination and explainability are already established? The answer was task-dependent, but the full sensor set was not always best. In RD, the best single segment was the right hand (balanced accuracy 0.746), while the best three-segment subset—right hand plus both lower legs—reached 0.947. This was higher than the full 10-segment configuration, which reached 0.886. In RGS, the best single segment was the left lower leg (0.731), the best three-segment subset (left foot, left lower leg, pelvis) reached 0.861, and the best four-segment subset (right foot, right hand, left lower leg, sternum) reached 0.917, again higher than the full 9-segment configuration (0.824).

 doi:10.20944/preprints202604.1435.v1

These results suggest two main points. First, a full sensor suit is not always needed, which is important for wearable system deployment. Second, the best subset depends on the task and may include compensatory signals outside the main working limb. Figure 5 shows the performance frontier across sensor counts, and Table 3 lists the corresponding best subsets.

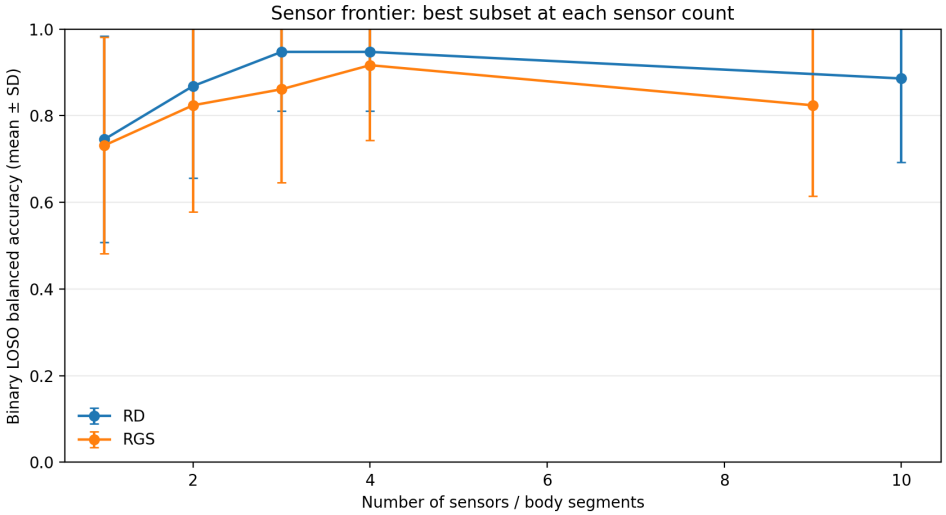

Figure 5. Performance of the best sensor subset at each subset size. For every possible number of sensors, the figure shows the subset that achieved the highest LOSO balanced accuracy (mean ± SD). For RD, the highest balanced accuracy was 0.947, achieved with Hand Right + LowerLeg Left + LowerLeg Right, and matched by a 4-sensor subset including Foot Left. For RGS, the highest balanced accuracy was 0.917, achieved with Foot Right + Hand Right + LowerLeg Left + Sternum. The exact sensor combinations are provided in Table 3. These results show that the optimal sensor configuration depends on the task.

Table 3. Best-performing unconstrained sensor subsets at each sensor count.

Task	k	Best Subset	Accuracy	Balanced acc.
RD	1	Hand Right	0.829	0.746
RD	2	Hand Right + LowerLeg Right	0.908	0.868
RD	3	Hand Right + LowerLeg Left + LowerLeg Right	0.947	0.947
RD	4	Foot Left + Hand Right + LowerLeg Left + LowerLeg Right	0.947	0.947
RD	All	Full 10-segment set	0.908	0.886
RGS	1	LowerLeg Left	0.847	0.731
RGS	2	Foot Right + LowerLeg Left	0.875	0.824
RGS	3	Foot Left + LowerLeg Left + Pelvis	0.903	0.861
RGS	4	Foot Right + Hand Right + LowerLeg Left + Sternum	0.903	0.917
RGS	All	Full 9-segment set	0.847	0.824

3.4. Lower-Body-Only Sensor Sets

Because some of the best unconstrained solutions included upper-body signals, we also examined lower-body-only subsets. This gave a more practical picture. For RD, performance improved as lower-body sensors were added, reaching balanced accuracy 0.702 with four segments (both lower legs and both upper legs). For RGS, performance remained strong with a compact lower-body setup: a three-segment subset consisting of left foot, left lower leg, and pelvis reached balanced accuracy 0.861, and a four-segment subset with right foot, both lower legs, and pelvis reached 0.870.

The contrast between tasks is informative. RD benefited more from signals outside the lower body, while RGS worked well with a compact lower-body setup. This suggests that sensor placement should be chosen based on the task and the intended use case, not as one fixed rule for all movements. Table 4 summarizes the lower-body-only results.

 doi:10.20944/preprints202604.1435.v1

Table 4. Best-performing lower-body-only subsets.

Task	k	Best Lower-Body Subset	Accuracy	Balanced acc.
RD	1	LowerLeg Right	0.750	0.593
RD	2	LowerLeg Right + UpperLeg Right	0.776	0.640
RD	3	LowerLeg Left + LowerLeg Right + UpperLeg Right	0.803	0.675
RD	4	LowerLeg Left + LowerLeg Right + UpperLeg Left + UpperLeg Right	0.816	0.702
RGS	1	LowerLeg Left	0.847	0.731
RGS	2	Foot Right + LowerLeg Left	0.875	0.824
RGS	3	Foot Left + LowerLeg Left + Pelvis	0.903	0.861
RGS	4	Foot Right + LowerLeg Left + LowerLeg Right + Pelvis	0.889	0.870

3.5. Proof-of-Concept Closed-Loop Extension Results

The next question was narrower: if the same feature space is viewed as a stream of short windows rather than full trials, does it still support a plausible corrective-feedback workflow? The answer was cautiously positive. Window-level discrimination remained above chance in both tasks and did not disappear when compact subsets were used. In RD, the full configuration reached window-level balanced accuracy 0.601 and the best compact three-segment setup reached 0.605. In RGS, the full configuration reached 0.593, while the compact and lower-body setups remained lower but still above chance (both about 0.527). These values are lower than the subject-level results, which is expected because short windows provide less information than full repetitions, but they are still sufficient to justify a proof-of-concept real-time framing.

The second closed-loop result was timing. Incorrect repetitions were often detected early rather than only near trial completion. Median first-detect progress was about 0.093 of the repetition in RD and about 0.047 in RGS, with essentially the same timing for the compact RD setup and the compact or lower-body RGS setups. In practical terms, the model often crossed into "incorrect" territory within the first 5–10% of the movement. This does not prove a finished real-time system, but it does show that the signal emerges early enough to make simulated feedback timing a meaningful research question.

The window-level explanation summaries were also consistent with the subject-level findings. At the variant level, RD pronation was most often linked to `right lower-leg mean speed higher`, RD supination to `right lower-leg rotational range higher`, RD toes to `right-hand mean speed higher`, RGS abduction to `pelvis mean speed higher`, RGS flexion to `left lower-leg RMS acceleration higher`, and RGS stork to `right upper-leg mean speed higher`. This matters because the explanation layer did not collapse when the task was reformulated in windows; it still pointed to concrete segment-feature deviations that could be mapped to a cue.

The feedback-trigger simulation needed more care. A permissive default rule produced too many triggers on correct repetitions and would have been difficult to defend. After tuning the policy to require higher confidence and persistent explanation patterns, false cueing dropped sharply. In RD, the tuned trigger fired in 9.4% of correct repetitions and 61.0% of incorrect repetitions, with median trigger progress 0.690 for correct repetitions and 0.277 for incorrect repetitions. In RGS, the corresponding values were 8.8% and 62.2%, with median trigger progress 0.619 for correct repetitions and 0.233 for incorrect repetitions. In other words, the conservative rule did not eliminate incorrect-trial cueing, but it made the proof-of-concept policy much less noisy on correct movement. Table 5 summarizes this added layer.

 doi:10.20944/preprints202604.1435.v1

Table 5. Proof-of-concept results for a real-time feedback version of the system. The upper part of the table shows how accurately movement errors can be detected from short time windows using three sensor setups (full, compact, and lower-body only). The lower part shows the performance of the final feedback rule, including the timing of the first corrective alert, the trigger rate on incorrect repetitions, and the false-trigger rate on correct repetitions.

Task	Configuration	Sensors	Window acc.	Window bal. acc.	Median First Detect	Trigger Rate
RD	Full	10	0.772	0.601	0.093	—
RD	Best compact	3	0.800	0.605	0.093	—
RD	Best lower-body	4	0.783	0.557	0.091	—
RGS	Full	9	0.792	0.593	0.047	—
RGS	Best compact	4	0.781	0.527	0.047	—
RGS	Best lower-body	3	0.781	0.527	0.047	—
RD	Tuned trigger, incorrect reps	10*	—	—	0.277†	0.610
RD	Tuned trigger, correct reps	10*	—	—	0.690†	0.094
RGS	Tuned trigger, incorrect reps	9*	—	—	0.233†	0.622
RGS	Tuned trigger, correct reps	9*	—	—	0.619†	0.088

* The tuned trigger was evaluated on the full-sensor prediction stream. The compact and lower-body configurations are shown in the upper part of the table for the window-level detection comparison. † For tuned-trigger rows, this column reports the median progress of the first feedback trigger among repetitions where a trigger occurred.

4. Discussion

The main contribution of this study is the obtained result that movement quality can be separated reliably even with a reduced and task-aware IMU configuration. In both benchmark tasks, the sensor-derived feature space preserved enough structure to distinguish correct from altered execution, and in some cases compact subsets performed as well as, or better than, the full configuration. This places the present study within a well-established rehabilitation literature showing that wearable inertial sensing can support exercise recognition and movement assessment outside highly instrumented laboratory settings. It also extends that literature toward a more explicit quality-oriented and deployment-aware formulation [14,16,17,22,23].

This positioning matters because much of the existing wearable rehabilitation literature has focused either on detecting which exercise is being performed or on monitoring adherence to prescribed activity. Those are important goals, but they are not identical to deciding whether a movement is performed correctly and then expressing that distinction in a way that can guide interpretation or feedback. Reviews of lower-limb exercise assessment and rehabilitation wearables show that the field has grown quickly, but they also note the limited number of user evaluation studies and the gap between technical performance and clinically useful deployment [17,18,22]. In that context, the present study is better understood not simply as another activity-classification study, but as a benchmark for interpretable movement-quality assessment with practical sensor reduction in mind [18,23].

A second important finding is that explanation can remain close to the measured signal space. In this study, the strongest discriminative patterns remain visible at the segment-feature level rather than being buried in a latent representation that is difficult to interpret. That is important because explainability in healthcare is valuable only if it helps human users understand what changed and why that change matters. More generally, the healthcare AI literature argues that interpretable outputs are important for trust, accountability, and practical decision support, not merely for model inspection [21]. Our results therefore suggest a useful middle ground: a simple model can support both classification and readable explanation when the representation itself remains biomechanically meaningful [21].

A third contribution is methodological rather than purely predictive. The study suggests that sensor reduction should not be treated only as a hardware simplification problem, but also as a representation problem. Earlier rehabilitation work has already shown that a single sensor, or a small number of sensors, can be sufficient for certain exercise recognition tasks [14,15,20]. Our results build

 doi:10.20944/preprints202604.1435.v1

on that direction by showing that reduced setups can still preserve enough information not only for discrimination, but also for explanation. This is especially relevant for movement monitoring systems intended for repeated use, home-based follow-up, or edge deployment, where setup burden and ease of use often matter as much as raw model capacity [22,23,25].

The proof-of-concept closed-loop extension also helps position the study relative to the broader rehabilitation technology literature. Prior studies have highlighted the need for sensor-based systems that do more than store recordings and instead support home rehabilitation, adherence monitoring, and timely feedback [14,16,19,25]. The present study does not yet deliver a validated real-time clinical feedback system, but it does show that the ingredients for such a system can be organized coherently: reduced sensing, early signal emergence, simple classification, and explanation in readable terms. In that sense, the study begins to bridge the gap between offline benchmarking and action-oriented monitoring [19,23].

Taken together, these findings support a broader practical principle: more sensing is not automatically more useful. In wearable rehabilitation, the goal is rarely to reconstruct everything that can be measured. It is to capture the subset of signals that best supports a clinically meaningful judgement. The literature increasingly points in this direction, emphasizing not only technical accuracy but also usability, interpretability, and translational fit in real settings [17,22,24]. From that perspective, reduced complexity is not a weakness of the approach. It is part of its intended value.

This study also has some limitations. First, the analysis is based on a relatively small cohort and on instructed movement deviations under controlled conditions. This makes the dataset suitable as a benchmark, but it does not capture the wider variability seen in clinical populations, where compensatory behaviour, fatigue, pain, and day-to-day inconsistency can alter movement quality in less structured ways [4,11]. Second, the modeling approach was intentionally simple. Logistic regression supports transparency, but it does not test whether more complex models would improve classification or whether explanation quality would remain as readable under richer model classes. Third, the study focuses on benchmarking rather than full system validation. Sensor subset selection, performance estimation, explanation generation, and the feedback extension were all explored within the same experimental framework. Finally, the readable summaries and closed-loop logic were not evaluated by clinicians or patients. Future work should therefore move beyond technical feasibility and test whether the proposed outputs improve understanding, decision-making, or follow-up in real rehabilitation workflows [21,25].

5. Conclusions

This study presents a novel ML-based framework of wearables-enhanced analytics and movement-quality assessment that distinguishes correct from altered movement using interpretable IMU features. The findings show that a restricted subset of meaningful signals is adequate for distinguishing correct from incorrect/altered movement, support interpretable analysis of movement deviations, and remain effective under reduced sensor configurations. In addition, the same feature set enable a proof-of-concept extension toward early error detection and corrective feedback. Overall, the proposed approach supports the development of wearables-enhanced rehabilitation systems that are accurate, interpretable, and practical for real-world use.

Author Contributions: Conceptualization, G.B. and G.S.; methodology, G.B.; software, G.B.; formal analysis, G.B.; investigation, G.B., G.S., and E.K.; writing—original draft preparation, G.B.; writing—review and editing, G.B., G.S., E.K., and K.K.; supervision, G.B. and K.K. All authors have read and agreed to the published version of the manuscript.

Funding: This research received no external funding.

Institutional Review Board Statement: Not applicable for this secondary analysis of an open dataset.

Informed Consent Statement: Not applicable for this secondary analysis of an open dataset.

 doi:10.20944/preprints202604.1435.v1

Data Availability Statement: The GAITEX dataset is publicly available from its original source publication and repository (DOI: 10.5281/zenodo.15729055), licensed under Creative Commons Attribution 4.0 International (CC BY 4.0).

Acknowledgments: The authors thank the creators of the GAITEX dataset for making the recordings publicly available.

Conflicts of Interest: The authors declare no conflicts of interest.

References

1. Celik, Y.; Stuart, S.; Woo, W. L.; Godfrey, A. Gait analysis in neurological populations: Progression in the use of wearables. *Med. Eng. Phys.* **2021**, *87*, 9–29. https://doi.org/10.1016/j.medengphy.2020.11.005.
2. Horst, F.; Lapuschkin, S.; Samek, W.; Müller, K.-R.; Schöllhorn, W. I. On the explainability of classification decisions with deep learning models in human movement analysis. In *Proceedings of the 42nd German Conference on Pattern Recognition*, Dortmund, Germany, 24–27 September 2019; Springer: Cham, Switzerland, 2019; pp. 15–28.
3. Jatesiktat, P.; Lim, G. M.; Kuah, C. W. K.; Anopas, D.; Ang, W. T. Autonomous modeling of repetitive movement for rehabilitation exercise monitoring. *BMC Med. Inform. Decis. Mak.* **2022**, *22*, 175. https://doi.org/10.1186/s12911-022-01907-5.
4. Spilz, A.; Oppel, H.; Werner, J.; Stucke-Straub, K.; Capanni, F.; Munz, M. GAITEX: Human motion dataset of impaired gait and rehabilitation exercises using inertial and optical sensors. *Sci. Data* **2026**, *13*, 11. https://doi.org/10.1038/s41597-025-06439-x.
5. Munz, M.; Spilz, A.; Oppel, H. *Dataset GAITEX: Human motion dataset of impaired gait and rehabilitation exercises using inertial and optical sensors* (1.0.0) [Data set]. Zenodo, 2025. https://doi.org/10.5281/zenodo.15729056.
6. Xsens. *Motion Capture*. Available online: https://www.xsens.com/products/motion-capture (accessed on 11 April 2026).
7. Papi, E.; Murtagh, G.M.; McGregor, A.H. Wearable technologies in osteoarthritis and rehabilitation: A systematic review. *Sensors* **2022**, *22*, 2243. https://doi.org/10.3390/s22062243.
8. Peake, J.M.; Kerr, G.; Sullivan, J.P. A critical review of consumer wearables, mobile applications, and equipment for providing biofeedback, monitoring stress, and sleep in physically active populations. *Front. Physiol.* **2018**, *9*, 743. https://doi.org/10.3389/fphys.2018.00743.
9. Amann, J.; Blasimme, A.; Vayena, E.; Frey, D.; Madai, V.I. Explainability for artificial intelligence in healthcare: A multidisciplinary perspective. *BMC Med. Inform. Decis. Mak.* **2020**, *20*, 310. https://doi.org/10.1186/s12911-020-01332-6.
10. Brennan, D.; Mawson, S.; Brownsell, S. Telerehabilitation: Enabling the remote delivery of healthcare, rehabilitation, and self-management. *Stud. Health Technol. Inform.* **2009**, *145*, 231–248.
11. Varoquaux, G. Cross-validation failure: Small sample sizes lead to large error bars. *NeuroImage* **2018**, *180*, 68–77. https://doi.org/10.1016/j.neuroimage.2017.06.061.
12. Amann, J.; Blasimme, A.; Vayena, E.; Frey, D.; Madai, V.I. Explainability for artificial intelligence in healthcare: A multidisciplinary perspective. *BMC Med. Inform. Decis. Mak.* **2020**, *20*, 310. https://doi.org/10.1186/s12911-020-01332-6.
13. Brennan, D.; Mawson, S.; Brownsell, S. Telerehabilitation: Enabling the remote delivery of healthcare, rehabilitation, and self-management. *Stud. Health Technol. Inform.* **2009**, *145*, 231–248.
14. Giggins, O.M.; Sweeney, K.T.; Caulfield, B. Rehabilitation exercise assessment using inertial sensors: A cross-sectional analytical study. *J. Neuroeng. Rehabil.* **2014**, *11*, 158. https://doi.org/10.1186/1743-0003-11-158.
15. Giggins, O.; Sweeney, K.T.; Caulfield, B. The use of inertial sensors for the classification of rehabilitation exercises. In *Proc. Annu. Int. Conf. IEEE Eng. Med. Biol. Soc.* **2014**, 2965–2968. https://doi.org/10.1109/EMBC.2014.6944245.
16. Huang, B.; Giggins, O.; Kechadi, T.; Caulfield, B. The limb movement analysis of rehabilitation exercises using wearable inertial sensors. In *Proc. Annu. Int. Conf. IEEE Eng. Med. Biol. Soc.* **2016**, 4686–4689. https://doi.org/10.1109/EMBC.2016.7591773.
17. Porciuncula, F.; Roto, A.V.; Kumar, D.; Davis, I.; Roy, S.; Walsh, C.J.; Awad, L.N. Wearable movement sensors for rehabilitation: A focused review of technological and clinical advances. *PM&R* **2018**, *10*, S220–S232. https://doi.org/10.1016/j.pmrj.2018.06.013.
18. Giggins, O.M.; Persson, U.M.; Caulfield, B. Wearable inertial sensor systems for lower limb exercise detection and evaluation: A systematic review. *Sports Med.* **2018**, *48*, 1221–1246. https://doi.org/10.1007/s40279-018-0878-4.

 doi:10.20944/preprints202604.1435.v1

19. Bavan, L.; Surmacz, K.; Beard, D.; Mellon, S.; Rees, J. Adherence monitoring of rehabilitation exercise with inertial sensors: A clinical validation study. *Gait Posture* **2019**, *70*, 211–217. https://doi.org/10.1016/j.gaitpost.2019.03.008.
20. Brennan, L.; Bevilacqua, A.; Kechadi, T.; Caulfield, B. Segmentation of shoulder rehabilitation exercises for single and multiple inertial sensor systems. *J. Rehabil. Assist. Technol. Eng.* **2020**, *7*, 2055668320915377. https://doi.org/10.1177/2055668320915377.
21. Amann, J.; Blasimme, A.; Vayena, E.; Frey, D.; Madai, V.I. Explainability for artificial intelligence in healthcare: A multidisciplinary perspective. *BMC Med. Inform. Decis. Mak.* **2020**, *20*, 310. https://doi.org/10.1186/s12911-020-01332-6.
22. Regterschot, G.R.H.; Ribbers, G.M.; Bussmann, J.B.J. Wearable movement sensors for rehabilitation: From technology to clinical practice. *Sensors* **2021**, *21*, 4744. https://doi.org/10.3390/s21144744.
23. Phan, V.; Song, K.; Silva, R.S.; Silbernagel, K.G.; Baxter, J.R.; Halilaj, E. Seven things to know about exercise classification with inertial sensing wearables. *IEEE J. Biomed. Health Inform.* **2024**, *28*, 3411–3421. https://doi.org/10.1109/JBHI.2024.3368042.
24. Shenoy, A.; Samra, M.S.; Van Ooteghem, K.; Beyer, K.B.; Thomson, S.; McIlroy, W.E.; Eng, J.J.; Pollock, C.L. Evaluating the usability of inertial measurement units for measuring and monitoring activity post-stroke: A scoping review. *Sensors* **2025**, *25*, 3694. https://doi.org/10.3390/s25123694.
25. Brennan, D.; Mawson, S.; Brownsell, S. Telerehabilitation: Enabling the remote delivery of healthcare, rehabilitation, and self-management. *Stud. Health Technol. Inform.* **2009**, *145*, 231–248.